Science of the Total Environment 656 (2019) 29–38

Contents lists available at ScienceDirect

Science of the Total Environment

journal homepage: www.elsevier.com/locate/scitotenv

Insight into complexation of Cu(II) to hyperthermophilic compost-derived humic acids by EEM-PARAFAC combined with heterospectral two dimensional correlation analyses

Jia Tang [a], Li Zhuang [b], Zhen Yu [a,*], Xiaoming Liu [a], Yueqiang Wang [a], Ping Wen [a,c], Shungui Zhou [c]

[a] Guangdong Key Laboratory of Integrated Agro-environmental Pollution Control and Management, Guangdong Institute of Eco-environmental Science & Technology, Guangzhou 510650, China
[b] Guangdong Key Laboratory of Environmental Pollution and Health, School of Environment, Jinan University, Guangzhou 510632, China
[c] Fujian Provincial Key Laboratory of Soil Environmental Health and Regulation, College of Resources and Environment, Fujian Agriculture and Forestry University, Fuzhou 350002, China

HIGHLIGHTS

- The interaction of Cu(II)-HAs was explored by PARAFAC coupled with hetero-2DCOS.
- Faster response of phenols led to better binding ability of HTC-HA with Cu(II).
- HTC was recommended to be applied in the remediation of Cu(II)-polluted soils.

GRAPHICAL ABSTRACT

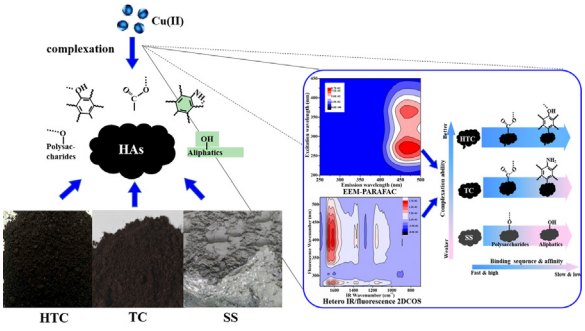

HAs: humic acids; HTC: hyperthermophilic compost; TC: thermophilic compost; SS: sewage sludge

ARTICLE INFO

Article history:
Received 14 September 2018
Received in revised form 23 November 2018
Accepted 24 November 2018
Available online 26 November 2018

Editor: Daniel CW Tsang

Keywords:
Hyperthermophilic compost
Humic acids
Cu(II) complexation
EEM-PARAFAC
Hetero-2DCOS

ABSTRACT

Hyperthermophilic composting has been demonstrated to overcome the disadvantages of conventional composting in products with better quality. However, the complexation of heavy metals to hyperthermophilic compost (HTC)-derived HA remains unclear. In the present work, using Cu(II) as the representative heavy metal, we investigated the binding process of Cu(II) to HAs derived from HTC, thermophilic compost (TC), and sewage sludge (SS). The complexation ability of three HAs was analyzed by the method of parallel factor (PARAFAC) coupled with hetero two-dimensional correlation spectroscopy (hetero-2DCOS) analyses. Results showed that HTC-derived HA has the greater complexation ability (log K_M = 5.68, CC_M = 1.21) than both TC-derived HA (log K_M = 5.27, CC_M = 0.94) and SS-derived HA (log K_M = 5.19, CC_M = 0.586), likely due to the higher humification degree, as well as the faster response of carboxyl and phenols to Cu(II) binding with HTC-derived HA. This study demonstrated that the utilization of HTC might provide an effective approach for remediation of Cu(II)-polluted soils. Moreover, PARAFAC analysis integrated with hetero-2DCOS offers a unique insight into understanding the correlation between HAs fractions and functional groups during the Cu(II) binding process.

1. Introduction

Since land application of sewage sludge becomes a promising waste utilization and disposal practice, it has been concerned as a potential

* Corresponding author at: Guangdong Institute of Eco-environmental Science & Technology, Guangzhou 510650, China.
E-mail address: yuzhen@soil.gd.cn (Z. Yu).

https://doi.org/10.1016/j.scitotenv.2018.11.357
0048-9697/

pathway of pollutants emission, in which the pollution of heavy metals in sewage sludge is one of the most important environmental issues (Mulchandani and Westerhoff, 2016; Yang et al., 2015). However, on the other hand, sewage sludge contains abundant dissolved organic matter (DOM) that is capable of directly participating the complexation process of heavy metals, consequently alleviate the pollution of heavy metals in soils (He et al., 2015; He et al., 2014a; He et al., 2014b; Wu et al., 2011). The complexation ability of DOMs with heavy metals is highly dependent on the structure and composition of DOMs. Humic-like substances have been demonstrated to exhibit better complexation ability than protein-like fractions (Huang et al., 2018; Chen et al., 2015; Wu et al., 2012a, b; Croué et al., 2003). As an important biological technology for treatment of sewage sludge, composting can transform organic materials into relatively stable humic substances, which has better complexation ability than sewage sludge (Marhuenda-Egea et al., 2007; Yu et al., 2010; Yamashita and Jaffé, 2008; He et al., 2014a, b; Sun et al., 2017; Huang et al., 2018).

Although composting product has advantages over sewage sludge in binding heavy metals, conventional composting is still limited in utilization due to the long composting period and unsatisfied compost quality (Macgregor et al., 1981; Zeng et al., 2010). Hyperthermophilic composting, an innovative technology, has been recently reported to overcome the disadvantages of conventional composting (Liao et al., 2018; Oshima and Moriya, 2008). Due to the distinctive thermophilic microbial community and a hyperthermophilic stage of ≥80 °C with the highest temperature exceeding 90 °C, hyperthermophilic composting significantly enhanced the maturity degree of compost product with a higher content of N and less antibiotic resistance genes and mobile genetic elements (Liao et al., 2018; Yu et al., 2018; Cui et al., 2019). Therefore, hyperthermophilic composting increasingly becomes a promising biotechnique for sewage sludge treatment and provides an ideal end-product as fertilizer or soil conditioner (Wei et al., 2018; Liao et al., 2018; Yuan et al., 2012). Since heavy metals pollution is one of the most important environmental issues in the land application of composting products, it is of great concern to assess desorption or complexation of heavy metals in composting product. However, to date, little is known about the complexation process of heavy metals to HAs derived from hyperthermophilic compost (HTC), the end-product from hyperthermophilic composting.

Diverse approaches are used to characterize the metal binding with DOMs or HAs, of which EEM-PARAFAC (Yuan et al., 2015; He et al., 2014a; Wu et al., 2011; Yamashita and Jaffé, 2008; Provenzano et al., 2004) and 2DCOS analyses (Huang et al., 2018; He et al., 2014b; Chen et al., 2015) are the most frequently used tools for metal-DOMs interaction analysis. He et al. (2014a) proved the better binding ability of humic-like fractions with heavy metals than protein-like fractions using EEM-PARAFAC analysis. Chen et al. (2015) employed IR/fluorescence hetero-2DCOS to obtain the sequential information of commercial HAs derived functional groups and fractions with Cu(II) binding. Huang et al. (2018) combined PARAFAC analysis and IR-2DCOS to determine the binding ability of different fractions and the sequential changes of functional groups in complexation of heavy metals. However, these reports did not illustrate the relationship between complexation ability of fractions and the response of functional groups to heavy metals binding with HAs.

As mentioned above, FTIR/fluorescence hetero-2DCOS can analysis the sequential response of functional groups and further determine the location of functional groups into different fractions, which could link the response of functional groups to the complexation ability of fractions quantified by EEM-PARAFAC analysis. Therefore, in the present work, using HA and Cu(II) as the representative DOM and heavy metal, respectively, we integrated EEM-PARAFAC and hetero-2DCOS analysis to provide an in-depth understanding of the binding characteristics of Cu(II) onto HTC-, TC-, and SS-derived HAs. We would figure out the contribution of response of functional groups to Cu(II) binding to complexation ability of different fractions at molecular level, in which the response of functional groups might play an important role in the complexation potential of different fractions and HTC-derived HA might exhibit a greater complexation ability than TC- and SS-derived HAs. This would offer a new perspective for analyzing the interaction of Cu(II)-HAs and the potential ability of HTC for the remediation of Cu(II)-polluted soils.

2. Material and methods

2.1. Sample preparation

The hyperthermophilic composting and conventional composting processes of sewage sludge were performed in a full-scale hyperthermophilic composting plant, which is located in Shunyi District, Beijing, China (40°03′10.48″N, 116°56′2.12″E). The detailed operational process of composting has been reported in our previous study (Yu et al., 2018). Two thoroughly mature compost samples, hyperthermophilic compost (HTC) and thermophilic compost (TC) were collected from these two composing processes after composted for 45 days. In addition, the composting raw material of sewage sludge (SS) was used as the initial sample. Three samples were air-dried, ground to pass through a 60-mesh sieve, and then utilized for the extraction of HAs as described by Zhang and Katayama (2012). The C, H, N and S contents of freeze-dried HAs were determined with an elementary analyzer (Elementar Vario EL, Germany), and the humic acid carbon (HAC) content was extracted and analyzed according to the methods described by Wang et al. (2014). The main characteristics and the metal contents of HAs derived from three samples are given in Table 1 and Table 2, respectively. Before titration, the extracted HAs were dissolved with distilled water, and the final concentrations of all HAs were diluted to 10 mg/L (as DOC concentration, pH 7.0). Metal titration was carried out by adding $CuCl_2$ titrants to 50 mL of HA solution in 100-mL brown sealed vials to generate a series of samples with Cu(II) concentration ranged from 0 to 180 μmol L^{-1} (0, 5, 10, 20, 40, 60, 80, 100, 140, and 180 μmol L^{-1}). During the titration process, the pH was maintained at 7.0 by adjusted with 0.1 mol L^{-1} NaOH or HCl solution. All titrated solutions were shaken at 25 °C in dark environment for 12 h to ensure equilibrium. Afterward, one part was analyzed by fluorescence EEM spectra and synchronous fluorescence spectra, and the rest was freeze dried for the FTIR spectroscopy analysis. The samples for determination of characteristics and titration were triplicates. And all the chemicals were purchased from Sinopharm Chemical Reagent Co., Ltd., China.

Table 1
Physico-chemical properties of extracted HAs isolated from hyperthermophilic compost (HTC), thermophilic compost (TC), and sewage sludge (SS) samples.

Samples	C%	N%	O%	H%	S%	Humic acid carbon %	DOC (mg/kg)
SS	53.93 ± 0.27[a]	7.22 ± 0.04	29.84 ± 0.22	6.33 ± 0.03	2.68 ± 0.04	1.92 ± 0.09	32.7 ± 1.6
TC	48.04 ± 0.07	8.28 ± 0.03	35.51 ± 0.08	5.33 ± 0.03	2.84 ± 0.05	2.33 ± 0.12	21.6 ± 0.7
HTC	47.34 ± 0.09	8.49 ± 0.03	36.34 ± 0.11	5.10 ± 0.05	2.73 ± 0.04	3.35 ± 0.08	19.4 ± 0.5

[a] The values presented in the columns are mean ± standard deviation ($n = 3$).

Table 2
The concentration of main heavy metals of extracted HAs derived from sewage sludge (SS), thermophilic compost (TC), and hyperthermophilic compost (HTC) samples.

Samples	Cu (mg/kg)	Cd (mg/kg)	Mn (mg/kg)	Pb (mg/kg)	Zn (mg/kg)
SS	282.14 ± 1.25[a]	1.01 ± 0.05	537.46 ± 15.08	34.19 ± 1.26	845.06 ± 29.94
TC	329.85 ± 10.31	1.29 ± 0.07	637.47 ± 13.53	43.63 ± 0.95	1002.98 ± 27.14
HTC	304.51 ± 2.6	1.25 ± 0.03	614.17 ± 9.89	40.1 ± 0.88	962.9 ± 37.71

[a] The values presented in the columns are mean ± standard deviation (n = 3).

2.2. Spectral determination of Cu(II) binding

EEM fluorescence spectra of HA with increasing Cu(II) concentration were obtained by a fluorescence spectrophotometer (Hitachi FP-7000, Japan) at room temperature. EEM spectra were obtained with measuring fluorescence intensity across emission wavelengths 250–550 nm and excitation wavelengths 200–450 nm with 5 nm increments. The slit widths of both the emission and excitation were set as 5 nm and the scanning speed was set at 2400 nm min^{-1}. Before analysis, the Raman and Rayleigh scatters were removed and adjusted by interpolation (He et al., 2014a).

Synchronous fluorescence spectra of titrated samples were carried out by a fluorescence spectrometer (Hitachi FP-7000, Japan). Synchronous-scan excitation spectra were obtained on a wavelength range of 250–550 nm with a constant offset (Dk = 18 nm) and 0.2 nm increments at a scan rate of 240 nm/min^{-1}.

For FTIR analysis, the mixtures of 2 mg freeze-dried HAs and 200 mg KBr (spectrometry grade) were ground and homogenized to reduce light scatter, and then pressed under 15 MPa for 2 min. FTIR spectra were obtained by using an Nicolet Nexus spectrometer (Thermo, USA) at 2 cm^{-1} resolution with scanning from 4000 to 400 cm^{-1}, and 64 scans were performed on each acquisition. It was noted that the region of 1750–700 cm^{-1} was chosen to be discussed below because the major bands of amide, carboxylic, phenolic, and carbohydrate functional groups were centrally included in this region (Chen et al., 2015).

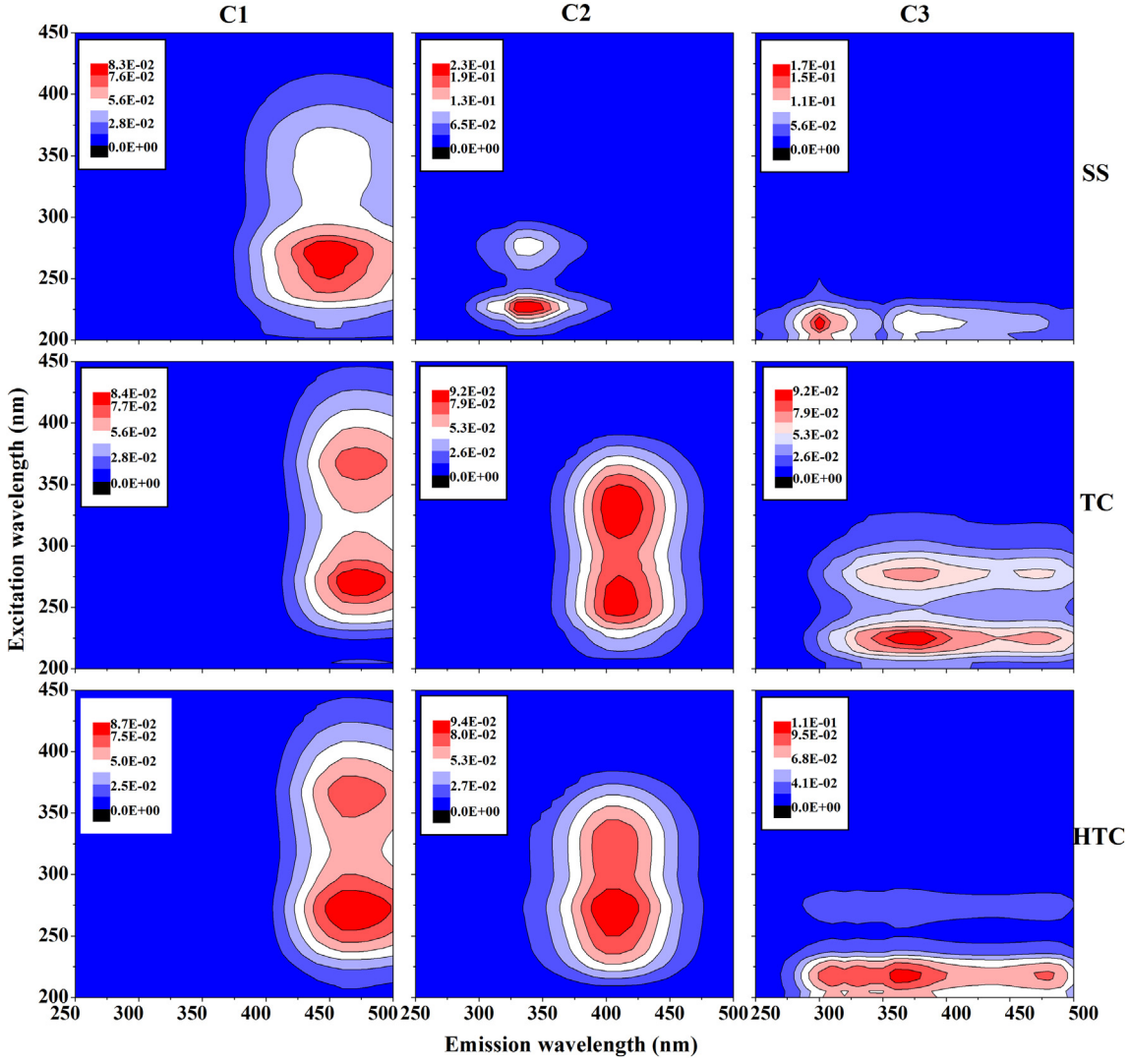

Fig. 1. Three fluorescence components (C1, C2, and C3) in HAs derived from sewage sludge (SS), thermophilic compost (TC), and hyperthermophilic compost (HTC) identified by EEM-PARAFAC analysis.

2.3. PARAFAC analysis and complexation modeling

According to the approach of Stedmon and Bro (2008), PARAFAC analysis was conducted using MATLAB 7.0 (Mathworks, USA) with the DOMFluor toolbox (www.models.life.du.dk). Two-seven component models were employed to compute PARAFAC data, and the fluorescence components were determined by the residual analysis, split half analysis and visual inspection. The maximum fluorescence intensity (F_{max}) (A.U.) was used to determine the relative abundance of individual components (Huang et al., 2018).

The complexation parameters between Cu(II) and PARAFAC-derived components were determined using the single-site fluorescence quenching model proposed by Ryan and Weber (1982), and the nonlinear fitting equation is as followed:

$$I = I_0 + (I_{ML} - I_0)\left(\frac{1}{2K_M C_L}\right) \times \left(1 + K_M C_L + K_M C_M - \sqrt{(1 + K_M C_L + K_M C_M)^2 - 4K_M^2 C_L C_M}\right)$$

where, I and I_0 are the fluorescence intensity at the metal concentration C_M and at the beginning of the titration (without adding metals), respectively. I_{ML} is the limiting value below which the fluorescence intensity does not change due to the metal addition. K_M and C_L are the conditional stability constant and total ligand concentration, respectively.

2.4. 2DCOS analysis

To obtain the structural variation information about complexation of Cu(II) to HA derived from different samples, 2DCOS was employed using FTIR and synchronous fluorescence spectra with Cu(II) concentration as the external perturbation. According to Noda and Ozaki (2004), 2DCOS spectra were produced using 2Dshige software (Kwansei-Gakuin University, Japan).

Spectral intensities and signs of related peaks in 2D spectra can be interpreted by the principles proposed by Noda and Ozaki (2004). In the synchronous map, auto-peaks with positive signs suggest spectral intensities, whereas cross-peaks represent the direction of the intensity change at the corresponding spectral coordinates. Asynchronous spectra present cross-peaks exclusively, in which the signs reveal the sequential order of the spectral intensity variations induced by the external perturbation. The same signs of the spectral coordinate (χ_1, χ_2) in both synchronous and asynchronous maps indicate that the spectral intensity change at χ_1 occurs prior to χ_2. The sequence of spectral change is reversed when the signs are opposite.

3. Results and discussion

3.1. Change in the fluorescence of HA fractions during titration of cu(II)

3.1.1. EEM-PARAFAC analysis showed different fractions among HTC-, TC-, and SS-derived HAs

EEM-PARAFAC analysis was applied to investigate the fluorescence of HAs fractions. As shown in Fig.1, three components were identified in each HA derived from different samples. According to the protocol of Chen et al. (2003), component 1 (C1) [Ex/Em = (270, 350)/450] was ascribed to humic-like fraction for SS-derived HA, while component 2 (C2) [Ex/Em = (228, 276)/337] and component 3 (C3) [Ex/Em = 214/(300, 370)] were classified as protein-like fractions. For TC-derived HA, C1 [Ex/Em = (271, 367)/472] and C2 [Ex/Em = (258, 329)/410] were assigned to humic-like fractions, and C3 [Ex/Em = (225, 277)/(377, 471)] was mainly ascribed to protein-like fraction with slight humic- and fulvic-like fraction. Similarly, for HTC-derived HA, C1 [Ex/Em = (273, 365)/467] and C2 [Ex/Em = (321, 271)/405] were classified as humic-like fractions, and C3 [Ex/Em = (218, 275)/(310, 329, 365, 479)] was mainly assigned to protein-like fraction with slight fulvic-like fraction. Sum of squared error for determining the components numbers and split half analysis for mode validation were presented in Fig. S1, which showed that three components were suitable for PARAFAC analysis.

PARAFAC analysis further displayed the quantitative information of the distribution of three components in all samples. For SS-derived HA, C2 (F_{max} = 750) was the most abundant constituent, followed by C3(F_{max} = 407) and C1 (F_{max} = 312). However, for compost-derived HAs, the highest level of three components was C1 (F_{max} = 957–961), and the contents of C3 (F_{max} = 222–380) were evidently lower than C1 and C2 (F_{max} = 783–792). These results demonstrated that protein-like fractions were abundant in sewage sludge-derived HA, whereas composting process enhanced the abundance of humic-like fractions at the expense of decreasing proteins. Similar phenomenon was also observed in the reports of Marhuenda-Egea et al. (2007) and Yu et al. (2010), which indicated that the humification process of composting significantly decreased the content of proteins but enriched the humic substances. In Table 1, the increasing N and O levels and decreasing H and C contents in compost-derived HAs also evidenced this humification process, which was due to oxidation, dehydrogenation and the formation of stable N containing compounds during composting. In addition, we noticed that the fluorescent intensity of C1 and C2 in HA derived from HTC were slightly higher than those from TC, suggesting

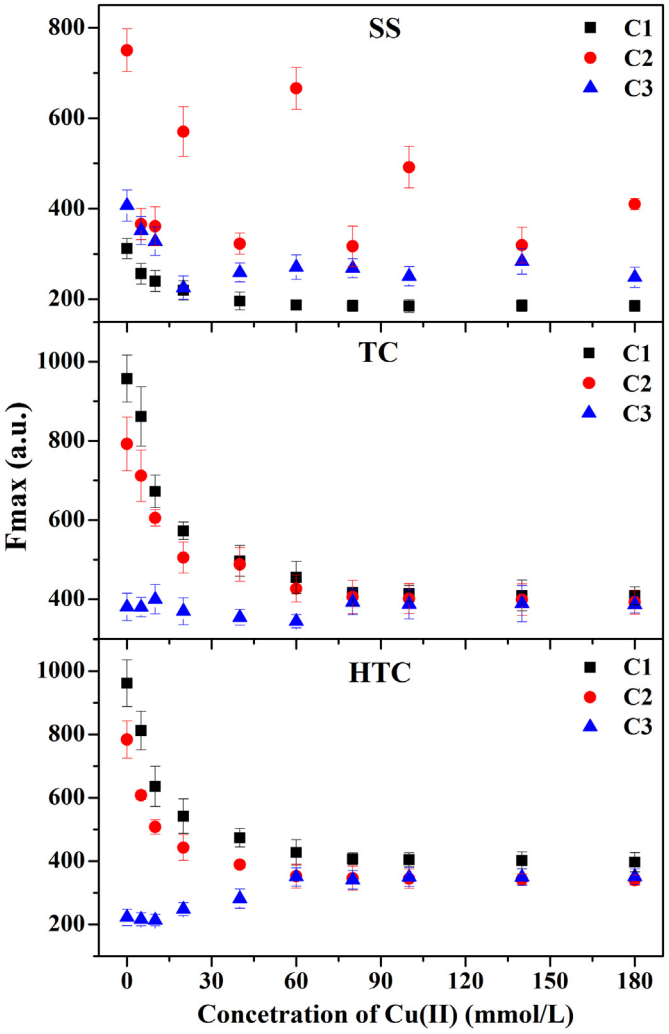

Fig. 2. Changes in fluorescence of different component of HAs derived from sewage sludge (SS), thermophilic compost (TC), and hyperthermophilic compost (HTC) during Cu(II) titration. Vertical bars represent the standard error of the mean values (n = 3).

Table 3
Fitting parameters of the Ryan-Weber Model of Cu(II) bound to C1, C2 and HAs derived from sewage sludge (SS), thermophilic compost (TC), and hyperthermophilic compost (HTC).

	HAs				C1				C2			
	Log K_M	R^2	I_{ML}	CC_M	Log K_M	R^2	I_{ML}	CC_M	Log K_M	R^2	I_{ML}	CC_M
SS	5.19	0.997	199.2	0.586	5.21	0.996	177.5	0.577	–	–	–	–
TC	5.27	0.995	648.3	0.940	5.26	0.995	384.4	0.733	5.14	0.988	375.7	1.08
HTC	5.68	0.992	621.0	1.21	5.35	0.995	380.1	0.996	5.29	0.994	327.2	1.33

that the level of humification in HTC-derived HA was higher than that in TC-derived HA. The 3.35% of humic acid carbon content in HTC was higher than TC, which strongly supported the above results.

3.1.2. Humic-like fractions exhibited stronger fluorescent quenching than protein-like fraction

Fig. 2 showed that the quenching curves of each fluorescence component with the addition of Cu(II) were different among three samples. The PARAFAC analysis showed remarkable decrease in fluorescence intensity of C1 and C2 for compost-derived HAs in response to the addition of Cu(II) with different concentrations, but negligible fluorescence quenching occurred in SS-derived HA. The dynamics of quenching curves was quite similar to that of commercial HA (Divya et al., 2009), landfill leachate-derived DOM (Wu et al., 2012a, b), other composts derived-DOMs (Huang et al., 2018; Hernández et al., 2006; Plaza et al., 2006a) and rice straw-derived DOM (Huang et al., 2018). As well, EEM spectra of Cu(II) bound to DOMs exhibited the similar regular patterns with the quenching curves (Fig. S2). The fluorescence intensity of HAs derived from both compost samples significantly decreased with the addition of Cu(II). The result indicated that compost-derived HAs bound Cu(II) with a higher complexation ability than SS-derived HA. Humic-like fractions were quenched significantly by Cu(II), which is

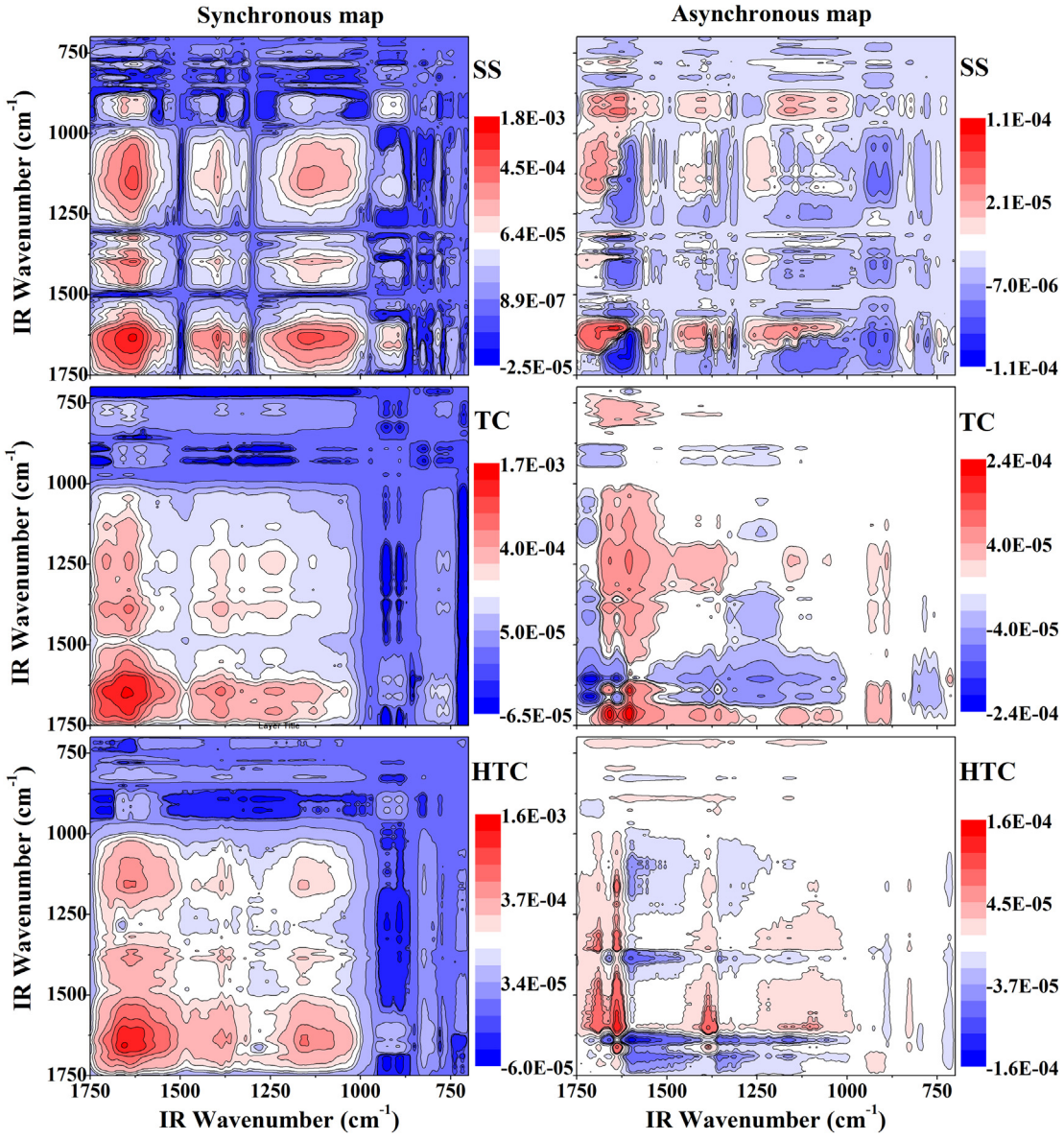

Fig. 3. Synchronous and asynchronous 2DCOS maps generated from the 1750–700 cm^{-1} regions of FTIR spectra for Cu(II) binding with HAs derived from sewage sludge (SS), thermophilic compost (TC) and hyperthermophilic compost (HTC).

consistent with previous reports describing the quenching effects of heavy metals on DOM derived from land leachates (Wu et al., 2011), composted municipal solid wastes and rice straw (Huang et al., 2018). However, compared with humic-like components, the quenching curves of protein-like substances with titration of Cu(II) were fluctuant in SS or maintained stable in compost samples. Similar phenomenon was also observed in some other studies (Huang et al., 2018; Yamashita and Jaffé, 2008). These results potentially suggested that the complexation ability of humic-like fractions with Cu(II) binding could be stronger than that of protein-like fractions, especially in compost samples.

3.1.3. HTC-derived HA presented better complexation ability than other HAs

The stability constants (log K_M) and complexing capacity (CC_M) calculated using Ryan and Weber model for humic-like fractions and HAs are listed in Table 3. As shown in Table 2, the Cu(II) concentrations of the three HAs were in the order of SS (282.14 ± 1.25 mg/kg) < HTC (304.51 ± 2.6 mg/kg) < TC (329.85 ± 10.31 mg/kg), indicating that the complexation potential of SS-derived HA could be greater than compost-derived HAs. However, the log K_M values of HAs were in the order of HTC (5.68) > TC (5.27) > SS (5.19), as well as the CC_M (Table 3). The log K_M values were 5.21, 5.26, and 5.35 for C1 in Cu(II) binding with HA derived from SS, TC, and HTC, respectively. The log K_M values in this work were in the same range as those calculated in water-extractable organic carbon derived from municipal solid waste and the composting product (5.09–5.97) (He et al., 2014a), humic acid from sewage sludge and sludge-amended soils (4.35–5.53) (Plaza et al., 2006b), and DOM derived from municipal solid waste (3.77–5.94) (Wu et al., 2011) and manure (3.87–5.03) (Huang et al., 2018). Besides, the CC_M value of C1 was the highest (0.996) in HTC, followed by TC (0.733) and SS (0.577). Similarly, the log K_M and CC_M values were also higher in HTC than in TC for C2. These results suggested that the composting process promoted the stability constants and complexing capacity of humic-like fractions with Cu(II) binding, which is consistent with the result of He et al. (2014a, b). More importantly, the complexing stability and capacity of HA binding with Cu(II) were greatly enhanced by hyperthermophilic composting, implying its advantage over sewage sludge and TC in application to Cu(II)-polluted soils.

3.2. Sequential response of functional groups and fractions to Cu(II) binding

2DCOS is a promising tool to improve the spectral resolution and solve the overlap problem by spreading spectrum in a second dimension, thus help us to obtain authentic details about the IR spectra changes of functional groups induced by the heavy metals binding (Chen et al., 2015; Cao et al., 2016). Although EEM-PARAFAC analysis presented the binding ability of individual HAs fraction with Cu(II), the correlation of response of functional groups to Cu(II) binding and the binding ability of individual fraction remains unknown. Hetero IR/fluorescence 2DCOS can provide the location of functional groups into different fractions, which could related the response of functional groups to Cu(II) binding to the complexation ability of individual fraction.

3.2.1. Carboxyl and phenols were the most sensitive functional groups for response to Cu(II) binding in HTC-derived HA

Fig. 3 showed the 2D IR-COS induced by complexation of Cu(II) to HAs derived from different samples. The predominant auto-peaks were obviously different among these HA samples. The synchronous maps showed 5 auto-peaks at 1560, 1395, 1324, 1137 and 1060 cm^{-1} in SS-derived HA, 6 auto-peaks at 1715, 1655, 1642, 1386, 1240, and 1055 cm^{-1} in TC-derived HA, and 5 auto-peaks at 1690, 1655, 1610, 1386, and 1160 cm^{-1} in HTC-derived HA. Except the bands smaller than 1000 cm^{-1}, most of auto-peaks in the synchronous maps were positive, indicating that signals of functional groups changed simultaneously with the increase of Cu(II) concentration. The peaks at 1137 cm^{-1} in SS-derived HA and 1610 cm^{-1} in HTC-derived HA were both separated into two peaks at 1164 and 1125 cm^{-1}, 1637 and 1599 cm^{-1} in asynchronous maps, respectively.

The 1715, 1607, 1599 and 1240 cm^{-1} signals can be attributed to the C═O or C—O stretching (or OH deformation) of carboxylic groups (Cao et al., 2016; Chen et al., 2015; He et al., 2011). The bands at 1690 and 1642 cm^{-1} are ascribed to the C═O stretching of amide (Chen et al., 2015; Liu et al., 2017). The bands at 1655 and 1637 cm^{-1} correspond

Table 4
2D-IR-COS results of the sign of each cross-peak in synchronous (Φ) and asynchronous (Ψ, in parentheses) maps for Cu(II) binding with HAs derived from sewage sludge (SS), thermophilic compost (TC), and hyperthermophilic compost (HTC).

	Sign[a]					
	SS					
	1631	1560	1395	1324	1125	1060
1560		+	+(−)	+(−)	+(−)	+(−)
1395			+	+(−)	+(−)	+(−)
1324				+	+(−)	+(−)
1125					+	+(−)
1060						+
	TC					
	1715	1658	1642	1386	1328	1055
1658		+	+(−)	+(−)	+(−)	+(−)
1642			+	+(−)	+(−)	+(−)
1386				+	+(−)	+(−)
1328					+	+(−)
1055						+
	HTC					
	1690	1637	1599	1384	1160	
1637		+	+(−)	+(−)	+(−)	
1599			+	+(+)	+(+)	
1384				+	+(+)	
1160					+	

[a] Signs were obtained in the upper-left corner of the maps: +, positive; −, negative.

to the aromatic C═C stretching (Li et al., 2011; He et al., 2011). The bands at 1395 and 1386 cm^{-1} are assigned to the phenolic OH deformation (He et al., 2011). The bands at 1164 and 1125 cm^{-1} can be ascribed to the aliphatic C—OH stretching (He et al., 2014b&2011). The bands at 1060 and 1055 cm^{-1} can be generated by the C—O stretching of polysaccharides (Chen et al., 2015; Li et al., 2011). The signs of cross-peaks in synchronous and asynchronous maps for complexation of Cu(II) with HAs are showed in Table 4. According to the sequential order rules (Noda and Ozaki, 2004), the change of functional groups of HA in SS binding with Cu(II) were sequenced as polysaccharides → aliphatics → amide → amines → phenols. While the sequence of functional groups changes in TC was as followed: carboxyl → amines → polysaccharides → phenolic OH → aromatic groups → amide. And the sequence of structural changes in HTC was in the order of carboxyl → phenolic OH → aliphatics → aromatic groups → amide. Compared with compost-derived HAs, polysaccharides and aliphatics provided the faster respond in SS sample. In compost samples, carboxyl was the most sensitive group to Cu(II) addition. This is consistent with the previous reports, which demonstrated that the carboxyl in DOM accounted for the high Cu(II) binding ability (He et al., 2014a&b; Xu et al., 2013). Besides carboxyl, phenols that could form highly stable ring structures with Cu (II) (Chen et al., 2015; Xu et al., 2013; Wu et al., 2012a, b) were also found to be the primary groups to participate Cu(II) complexation in HTC-derived HA. Phenols have been demonstrated to be important functional groups in composting process, in which the abundance of phenols was enriched with the increasing degree of humification (Traversa et al., 2010; Li et al., 2013). Therefore, the higher degree of humification in HTC than in TC could account for more phenols which were more susceptible to Cu(II) binding to HTC-derived HA as compared to TC.

3.2.2. Carboxyl and phenols were located in humic-like fractions in HTC-derived HA

Since fluorescence and IR spectra represent different structures of HA, we employed 2D heterospectral fluorescence/IR correlation analysis to verify the band assignments and the correspondence between these two techniques (Fig. 4). For SS-derived HA, there are 4 cross peaks located in the IR regions of 1631, 1164, 926, 896 cm^{-1} and the correspondence fluorescence regions of 383 and 280 nm in synchronous map. Five cross-peaks were located in the IR regions of 1715, 1642, 1386, 1328,

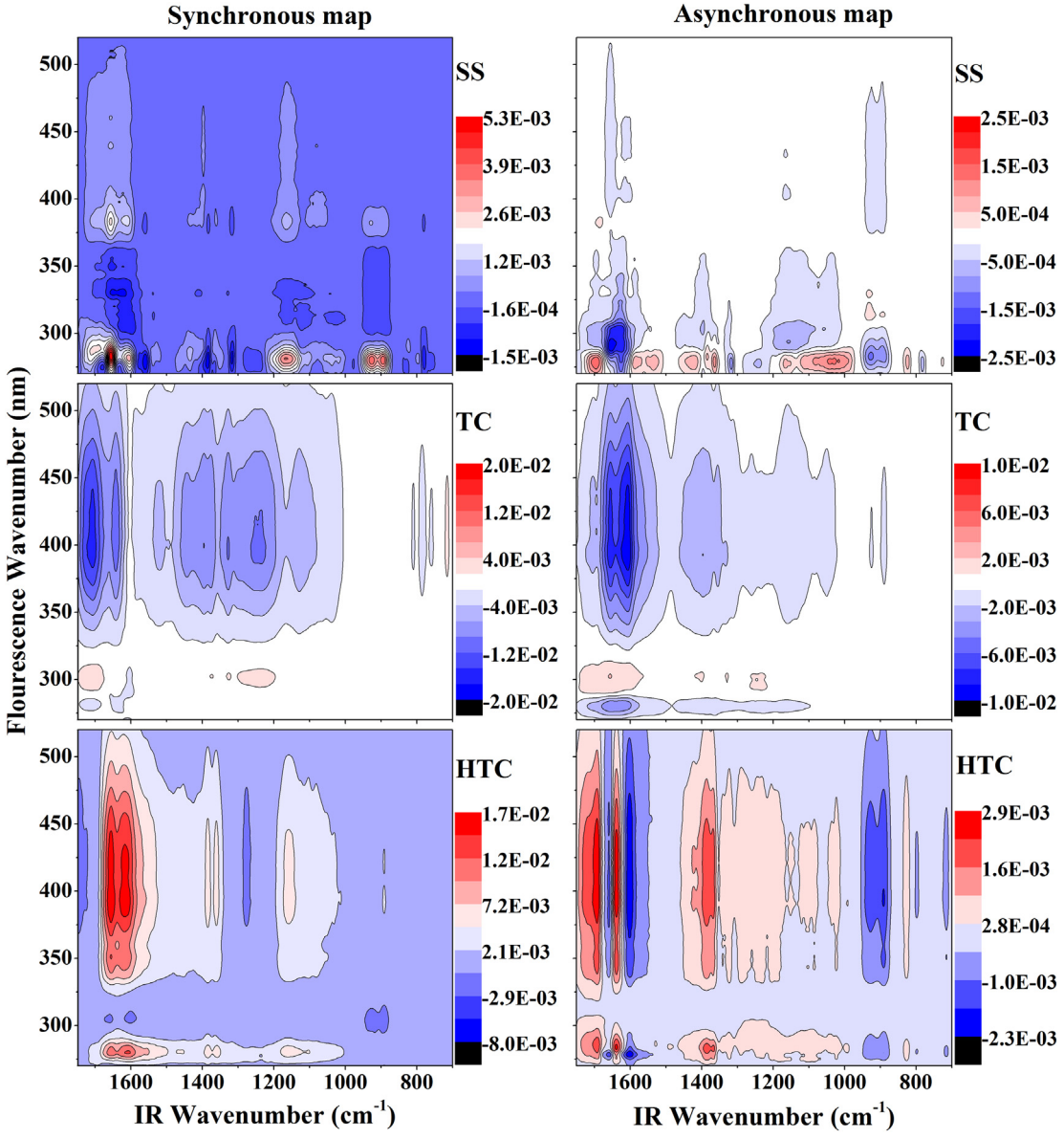

Fig. 4. Synchronous and asynchronous 2DCOS maps generated from the 250–550 nm regions of fluorescent spectra and 1750–700 cm^{-1} regions of FTIR spectra for Cu(II) binding with HAs derived from sewage sludge (SS), thermophilic compost (TC) and hyperthermophilic compost (HTC).

1240 m^{-1} and the correspondence fluorescence regions of 422, 393, and 280 nm for TC-derived HA in synchronous map. For HA derived from HTC, four cross-peaks were observed in the IR regions of 1658, 1637, 1384, and 1160 cm^{-1} and the correspondence fluorescence regions of 422, 395, and 280 nm. These cross-peaks showed positive signs in SS and HTC samples, but negative in TC samples. In asynchronous maps, the cross-peaks were divided into different parts. For SS-derived HA, groups at 1695, 1560, 1164, and 1125 cm^{-1} were related to protein-like fraction (280 nm). In TC sample, groups at 1658 cm^{-1} was ascribed to protein-fraction (280 nm), and groups at 1607 and 1386 cm^{-1} were related to humic-like fraction (393 nm). For HTC-derived HA, groups at 1637 and 1595 cm^{-1} corresponded to humic-like fraction (395 nm) and fulvic-like fraction (351 nm), and group at 1384 cm^{-1} was related to humic-like fraction (395 nm). These results indicated that carboxylic, aromatic, and phenolic groups were the basic fluorescent units for humic- or fulvic-like fractions, while protein-like fraction was related to amide, aliphatic groups, and some carbohydrates, which were consistent with the results from Chen et al. (2015) and He et al. (2015).

As mentioned in 2DCOS of IR, the asynchronous maps of hetero spectral 2DCOS also provided the sequential information about the changes of IR and fluorescence spectra. For SS-derived HA, at 280 nm, there were one negative sign at 1631 cm^{-1}, and four positive sign at 1695, 1560, 1164, and 1125 cm^{-1}, suggesting that the fluorescence response of protein-like fraction occurred before the spectral changes of aromatic group, and after the amide and aliphatic group. All of seven signs were negative in TC-derived HA, which indicated that the spectral changes of carboxylic, aromatic, and phenolic groups were observed before the fluorescent change of humic-like fraction. The sign of 1328 cm^{-1} located at 280 nm was positive, which suggested that the IR spectra of amine changed before the fluorescence quenching of protein-like substance. As well, for HTC-derived HA, the spectral intensity of carboxylic and phenolic groups changed before the fluorescence spectral change of humic- and fulvic-like fractions. Furthermore, for the band (280 nm) assigned with protein-like substance, the sign of 1160 cm^{-1} was positive in HTC-derived HA, suggesting that the IR spectral change of aliphatic group occurred before the fluorescence change of protein-like fraction.

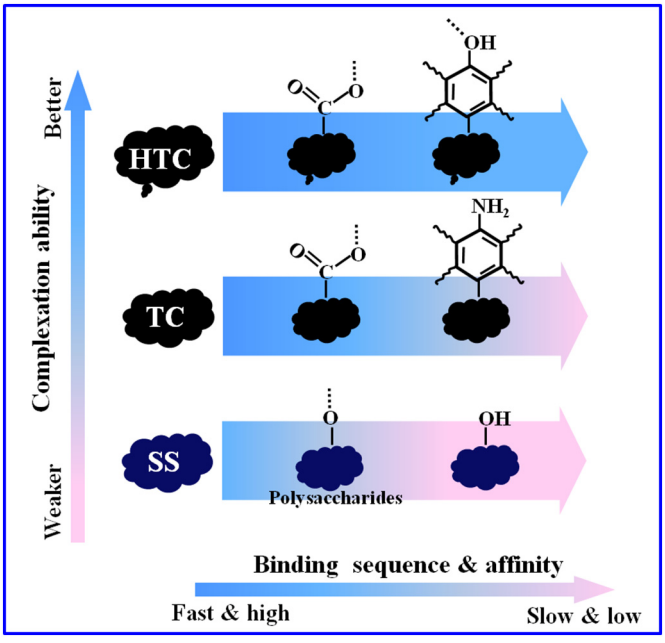

Fig. 5. Correlation of complexation abilities with sequential response of functional groups to Cu(II) binding with HAs.

3.3. The faster response of carboxyl and phenols to cu(II) binding accounted for the better complexation ability of humic-like fractions in HTC-derived HA

He et al. (2011 & 2014b) found that composting process enhanced the content of humic-like fractions, and led to the greater Cu(II) binding ability. In this work, compost-derived HAs showed greater complexation ability on Cu(II) binding than SS-derived HA. In addition, humic-like fractions of C1 and C2 have the higher complexation ability with Cu(II) than protein-like fraction of C3 in compost-derived HAs. We also found that the abundance of humic-like substances was significantly promoted by composting process, especially the hyperthermophilic composting. Moreover, the binding properties of heavy metals to DOMs or HAs not only depends on the composition, but also relies on the functional groups of DOM (Huang et al., 2018; Sun et al., 2017; Xu et al., 2013). Most of reports demonstrated that carboxyl and phenols in humic-like fraction of DOMs accounted for the high Cu(II) binding capacity and strong affinity (Huang et al., 2018; He et al. 2014a&b; Xu et al., 2013). In our work, the hetero-2DCOS analysis illustrated that carboxyl and phenols were the predominant groups in humic-like fraction. Therefore, composting products possessing the greater complexation ability with Cu(II) than SS was mainly due to the increased content of humic-like substances and the functional groups with stronger affinity, e.g. carboxylic and phenolic groups (Fig. 5). Moreover, the complexation ability of Cu(II) to HAs may be enhanced by the increase of humification degree.

Although the abundance of humic-like fractions and the related functional groups were close to each other in both compost-derived HAs, the binding capacity (log K_M) and stability (CC_M) of humic-like fractions in HTC-derived HA were higher than in TC-derived HA (Table 2). In fact, the sequences of functional groups of HAs with Cu (II) binding were significantly different between compost samples. In the HTC sample, carboxyl and phenol with high binding affinity which were classified to humic-like fractions, were the primary functional groups to bind Cu(II). Nevertheless, carboxyl and amines were the mainly groups for binding Cu(II) in the TC sample. This could be attributed to the higher degree of humification in HTC than that in TC, which resulted in more abundant phenols in HTC-derived HA. Some previous reports found that the enhancement of complexation ability of Cu(II) binding to DOMs could be related to the response of functional groups of DOMs (Huang et al., 2018; Sun et al., 2017; Chen et al., 2015; Xu et al., 2013). Therefore, we speculated that HTC with higher complexation ability as compared to TC could be mainly attributed to the higher humification degree, as well as the resulted more abundant phenols with the faster response to Cu(II) addition (Fig. 5).

3.4. Environmental implication

In China, with the development of urbanization, about 40 million tons of sewage sludge was generated in 2017 and the annual growth rate reached to 13%, causing serious environmental risks. Hyperthermophilic composting becomes a promising biotechnique with a higher composting efficiency for the treatment of sewage sludge and provides an end-product with better quality as fertilizer or soil conditioner (Yu et al., 2018; Liao et al., 2018). We further demonstrated the greater binding ability of HTC than TC by EEM-PARAFAC coupled with hetero-2DCOS analyses in the present work. Given these advantages mentioned above, the land utilization of HTC could be widespread for in situ remediation of Cu(II)-polluted soil, as well as many stabilizing effective agents used to treat and control heavy metals pollution, such as red mud (Zhou et al., 2017a), biochar (Zhou et al., 2017b), oxidized multiwalled carbon nanotube (Zhou et al., 2019). However, contaminants contained in composting products, such as toxic organic pollutants and heavy metals, are the major limitations to land application of compost. The analysis method in the present study could offer a unique insight into the passivation of heavy metals in the hyperthermophilic

composting process, which is necessary for the optimization of land application of composting product.

4. Conclusions

EEM-PARAFAC coupled with hetero-2DCOS analyses were used to elucidate the binding characteristics of Cu(II) with HAs derived from SS, TC, and HTC. HTC showed the higher humification degree and the resulted faster response of carboxyl and phenols to Cu(II) addition, which accounted for the greater complexing ability of HTC-derived HA ($\log K_M = 5.68$, $CC_M = 1.21$) than TC- ($\log K_M = 5.27$, $CC_M = 0.94$) and SS-derived HA ($\log K_M = 5.19$, $CC_M = 0.586$). The results suggested that compared with SS and TC, the utilization of HTC would be a more efficient approach for the remediation of Cu(II)-polluted soils. Furthermore, the analysis method might provide a new insight into the inner correlation of functional groups and fluorescent fractions in Cu(II)-HAs interactions.

Acknowledgement

This study was supported by the GDAS' Project of Science and Technology Development (2017GDASCX-0409); the National Natural Science Foundation of China (41501546); the National Key Research and Development Program of China (2017YFD0800902); the Natural Science Foundation of Guangdong Province, China (2018A030313443).

Appendix A. Supplementary data

Supplementary data to this article can be found online at https://doi.org/10.1016/j.scitotenv.2018.11.357.

References

Cao, X., Drosos, M., Leenheer, J.A., Mao, J., 2016. Secondary structures in a freeze-dried lignite humic acid fraction caused by hydrogen-bonding of acidic protons with aromatic rings. Environ. Sci. Technol. 50 (4), 1663–1669.

Chen, W., Westerhoff, P., Leenheer, J.A., Booksh, K., 2003. Fluorescence excitation-emission matrix regional integration to quantify spectra for dissolved organic matter. Environ. Sci. Technol. 37 (24), 5701–5710.

Chen, W., Habibul, N., Liu, X.Y., Sheng, G.P., Yu, H.Q., 2015. FTIR and synchronous fluorescence Heterospectral two-dimensional correlation analyses on the binding characteristics of copper onto dissolved organic matter. Environ. Sci. Technol. 49, 2052–2058.

Croué, J.P., Benedetti, M.F., Violleau, D., Leenheer, J.A., 2003. Characterization and copper binding of humic and nonhumic organic matter isolated from the South Platte River: evidence for the presence of nitrogenous binding site. Environ. Sci. Technol. 37, 328–336.

Cui, P., Chen, Z., Zhao, Q., Yu, Z., Yi, Z., Liao, H., Zhou, S., 2019. Hyperthermophilic composting significantly decreases N_2O emissions by regulating N_2O-related functional genes. Bioresour. Technol. 272, 433–441.

Divya, O., Venkataraman, V., Mishra, A.K., 2009. Analysis of metal ion concentration in humic acid by excitation emission matrix fluorescence and chemometric methods. J. Appl. Spectrosc. 76 (6), 864–875.

He, X.S., Xi, B., Wei, Z., Guo, X., Li, M., An, D., Liu, H., 2011. Spectroscopic characterization of water extractable organic matter during composting of municipal solid waste. Chemosphere 82 (4), 541–548.

He, X.S., Xi, B.D., Pan, H.W., Li, X., Li, D., Cui, D.Y., Tang, W.B., Yuan, Y., 2014a. Characterizing the heavy metal-complexing potential of fluorescent waterextractable organic matter from composted municipal solid wastes using fluorescence excitation–emission matrix spectra coupled with parallel factor analysis. Environ. Sci. Pollut. R. 21, 7973–7984.

He, X.S., Xi, B.D., Zhang, Z.Y., Gao, R.T., Tan, W.B., Cui, D.Y., 2014b. Insight into the evolution, redox, and metal binding properties of dissolved organic matter from municipal solid wastes using two-dimensional correlation spectroscopy. Chemosphere 117, 701–707.

He, X.S., Xi, B.D., Zhang, Z.Y., Gao, R.T., Tan, W.B., Cui, D.Y., Yuan, Y., 2015. Composition, removal, redox, and metal complexation properties of dissolved organic nitrogen in composting leachates. J. Hazard. Mater. 283, 227), 227–233.

Hernández, D., Plaza, C., Senesi, N., Polo, A., 2006. Detection of copper(II) and zinc(II) binding to humic acids from pig slurry and amended soils by fluorescence spectroscopy. Environ. Pollut. 143 (2), 212–220.

Huang, M., Li, Z., Huang, B., Luo, N., Zhang, Q., Zhai, X., Zeng, G., 2018. Investigating binding characteristics of cadmium and copper to DOM derived from compost and rice straw using EEM-PARAFAC combined with two-dimensional FTIR correlation analyses. J. Hazard. Mater. 344, 539–548.

Li, X., Xing, M., Yang, J., Huang, Z., 2011. Compositional and functional features of humic acid-like fractions from vermicomposting of sewage sludge and cow dung. J. Hazard. Mater. 185 (2–3), 740–748.

Li, X.W., Xing, M.Y., Yang, J., Zhao, L., Dai, X., 2013. Organic matter humification in vermifiltration process for domestic sewage sludge treatment by excitation-emission matrix fluorescence and Fourier transform infrared spectroscopy. J. Hazard. Mater. 261, 491–499.

Liao, H.P., Lu, X.M., Rensing, C., Friman, V.P., Geisen, S., Chen, Z., Yu, Z., Wei, Z., Zhou, S.G., Zhu, Y.G., 2018. Hyperthermophilic composting accelerates the removal of antibiotic resistance genes and mobile genetic elements in sewage sludge. Environ. Sci. Technol. 52, 266–276.

Liu, X.Y., Chen, W., Qian, C., Yu, H.Q., 2017. Interaction between dissolved organic matter and long-chain ionic liquids: a microstructural and spectroscopic correlation study. Environ. Sci. Technol. 51 (9), 4812–4820.

Macgregor, S.T., Miller, F.C., Psarianos, K.M., Finstein, M.S., 1981. Composting process control based on interaction between microbial heat output and temperature. Appl. Environ. Microbiol. 41, 1321–1330.

Marhuenda-Egea, F.C., Martínez-Sabater, E., Jordá, J., Moral, R., Bustamante, M.A., Paredes, C., Pérez-Murcia, M.D., 2007. Dissolved organic matter fractions formed during composting of winery and distillery residues: evaluation of the process by fluorescence excitation–emission matrix. Chemosphere 68, 301–309.

Mulchandani, A., Westerhoff, P., 2016. Recovery opportunities for metals and energy from sewage sludges. Bioresour. Technol. 215, 215–226.

Noda, I., Ozaki, Y. (Eds.), 2004. Two-dimensional Correlation Spectroscopy-Applications in Vibrational and Optical Spectroscopy. John Wiley, England.

Oshima, T., Moriya, T., 2008. A preliminary analysis of microbial and biochemical properties of high-temperature compost. Ann. N. Y. Acad. Sci. 1125, 338–344.

Plaza, C., Brunetti, G., Senesi, N., Polo, A., 2006a. Fluorescence characterization of metal ion-humic acid interactions in soils amended with composted municipal solid wastes. Anal. Bioanal. Chem. 386 (7–8), 2133–2140.

Plaza, C., Brunetti, G., Senesi, N., Polo, A., 2006b. Molecular and quantitative analysis of metal ion binding to humic acids from sewage sludge and sludge-amended soils by fluorescence spectroscopy. Environ. Sci. Technol. 40 (3), 917–923.

Provenzano, M.R., D'Orazio, V., Jerzykiewicz, M., Senesi, N., 2004. Fluorescence behavior of Zn and Ni complexes of humic acids from different sources. Chemosphere 55 (6), 885–892.

Ryan, D.K., Weber, J.H., 1982. Fluorescence quenching titration for determination of complexing capacities and stability constants of fulvic acid. Anal. Chem. 54, 986–990.

Stedmon, C.A., Bro, R., 2008. Characterizing dissolved organic matter fluorescence with parallel factor analysis: a tutorial. Limnol. Oceanogr. Methods 6, 572–579.

Sun, F., Polizzotto, M.L., Guan, D., Wu, J., Shen, Q., Ran, W., Wang, B., Yu, G., 2017. Exploring the interactions and binding sites between Cd and functional groups in soil using two-dimensional correlation spectroscopy and synchrotron radiation based spectromicroscopies. J. Hazard. Mater. 326, 18–25.

Traversa, A., Loffredo, E., Gattullo, E., Senesi, N., 2010. Water-extractable organic matter of different compost: a comparative study of properties and allelochemical effects on horticultural plants. Geoderma 156, 287–292.

Wang, C., Tu, Q., Dong, D., Strong, P.J., Wang, H., Sun, B., Wu, W., 2014. Spectroscopic evidence for biochar amendment promoting humic acid synthesis and intensifying humification during composting. J. Hazard. Mater. 280, 409–416.

Wei, H.W., Wang, L.H., Hassan, M., Xie, B., 2018. Succession of the functional microbial communities and the metabolic functions in maize straw composting process. Bioresour. Technol. 256, 333–341.

Wu, J., Zhang, H., He, P.J., Shao, L.M., 2011. Insight into the heavy metal binding potential of dissolved organic matter in MSW leachate using EEM quenching combined with PARAFAC analysis. Water Res. 45, 1711–1719.

Wu, J., Zhang, H., Shao, L.M., He, P.J., 2012a. Fluorescent characteristics and metal binding properties of individual molecular weight fractions in municipal solid waste leachate. Environ. Pollut. 162, 63–71.

Wu, J., Zhang, H., Yao, Q.S., Shao, L.M., He, P.J., 2012b. Toward understanding the role of individual fluorescent components in DOM-metal binding. J. Hazard. Mater. 215, 294–301.

Xu, H., Yu, G., Yang, L., Jiang, H., 2013. Combination of two-dimensional correlation spectroscopy and parallel factor analysis to characterize the binding of heavy metals with DOM in lake sediments. J. Hazard. Mater. 263, 412–421.

Yamashita, Y., Jaffé, R., 2008. Characterizing the interactions between trace metals and dissolved organic matter using excitation−emission matrix and parallel factor analysis. Environ. Sci. Technol. 42, 7374–7379.

Yang, G., Zhang, G.M., Wang, H.C., 2015. Current state of sludge production, management, treatment and disposal in China. Water Res. 78, 60–73.

Yu, G.H., Luo, Y.H., Wu, M.J., Tang, Z., Liu, D.Y., Yang, X.M., Shen, Q.R., 2010. PARAFAC modeling of fluorescence excitation–emission spectra for rapid assessment of compost maturity. Bioresour. Technol. 101, 8244–8251.

Yu, Z., Tang, J., Liao, H., Liu, X., Zhou, P., Chen, Z., Christopher, R., Zhou, S., 2018. The distinctive microbial community improves composting efficiency in a full-scale hyperthermophilic composting plant. Bioresour. Technol. 265, 146–154.

Yuan, Y., Tao, Y., Zhou, S.G., Yuan, T., Lu, Q., He, J., 2012. Electron transfer capacity as a rapid and simple maturity index for compost. Bioresour. Technol. 116, 428–434.

Yuan, D.H., Guo, X.J., Wen, L., He, L.S., Wang, J.G., Li, J.Q., 2015. Detection of Copper (II) and Cadmium (II) binding to dissolved organic matter from macrophyte decomposition by fluorescence excitation-emission matrix spectra combined with parallel factor analysis. Environ. Pollut. 204, 152–160.

Zeng, G.M., Yu, M., Chen, Y.N., Huang, D.L., Zhang, J.C., Huang, H.L., Jiang, R.Q., Yu, Z., 2010. Effects of inoculation with *Phanerochaete chrysosporium* at various time points on enzyme activities during agricultural waste composting. Bioresour. Technol. 101, 222–227.

Zhang, C.F., Katayama, A., 2012. Humin as an electron mediator for microbial reductive dehalogenation. Environ. Sci. Technol. 46, 6575–6583.
Zhou, R., Liu, X., Luo, L., Zhou, Y., Wei, J., Chen, A., Tang, L., Wu, H., Deng, Y., Zhang, F., Wang, Y., 2017a. Remediation of cu, Pb, Zn and cd-contaminated agricultural soil using a combined red mud and compost amendment. Int. Biodeterior. Biodegrad. 118, 73–81.
Zhou, Y., Liu, X., Xiang, Y., Wang, P., Zhang, J., Zhang, F., Wei, J., Luo, L., Lei, M., Tang, L., 2017b. Modification of biochar derived from sawdust and its application in removal of tetracycline and copper from aqueous solution: adsorption mechanism and modelling. Bioresour. Technol. 245, 266–273.
Zhou, Y., He, Y., Xiang, Y., Meng, S., Liu, X., Yu, J., Yang, J., Zhang, J., Qin, P., Luo, L., 2019. Single and simultaneous adsorption of pefloxacin and Cu(II) ions from aqueous solutions by oxidized multiwalled carbon nanotube. Sci. Total Environ. 646, 29–36.